ACCOUNTS of chemical research

Article

Cite This: Acc. Chem. Res. XXXX, XXX, XXX−XXX

pubs.acs.org/accounts

Spectrally Resolved and Functional Super-resolution Microscopy via Ultrahigh-Throughput Single-Molecule Spectroscopy

Rui Yan,[†,∥] Seonah Moon,[†,∥] Samuel J. Kenny,[†,∥] and Ke Xu*[,†,‡,§]

[†]Department of Chemistry, University of California, Berkeley, California 94720, United States

[‡]Division of Molecular Biophysics and Integrated Bioimaging, Lawrence Berkeley National Laboratory, Berkeley, California 94720, United States

[§]Chan Zuckerberg Biohub, San Francisco, California 94158, United States

CONSPECTUS: As an elegant integration of the spatial and temporal dimensions of single-molecule fluorescence, single-molecule localization microscopy (SMLM) overcomes the diffraction-limited resolution barrier of optical microscopy by localizing single molecules that stochastically switch between fluorescent and dark states over time. While this type of super-resolution microscopy (SRM) technique readily achieves remarkable spatial resolutions of ∼10 nm, it typically provides no spectral information. Meanwhile, current scanning-based single-location approaches for mapping the positions and spectra of single molecules are limited by low throughput and are difficult to apply to densely labeled (bio)samples.

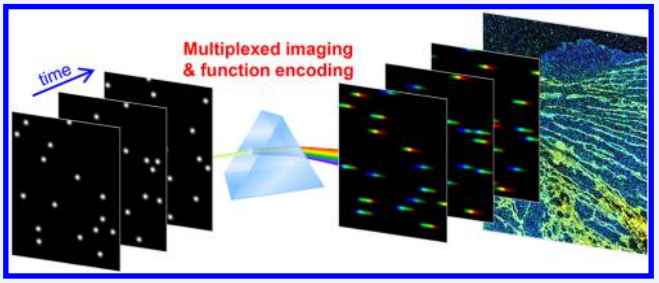

In this Account, we summarize the rationale, design, and results of our recent efforts toward the integration of the spectral dimension of single-molecule fluorescence with SMLM to achieve spectrally resolved SMLM (SR-SMLM) and functional SRM (*f*-SRM).

By developing a wide-field scheme for spectral measurement and implementing single-molecule fluorescence on−off switching typical of SMLM, we first showed that in densely labeled (bio)samples it is possible to record the fluorescence spectra and positions of millions of single molecules synchronously within minutes, giving rise to ultrahigh-throughput single-molecule spectroscopy and SR-SMLM. This allowed us to first show statistically that for many dyes, single molecules of the same species exhibit near identical emission in fixed cells. This narrow distribution of emission wavelengths, which contrasts markedly with previous results at solid surfaces, allowed us to unambiguously identify single molecules of spectrally similar dyes. Crosstalk-free, multiplexed SRM was thus achieved for four dyes that were merely 10 nm apart in emission spectrum, with the three-dimensional SRM images of all four dyes being automatically aligned within one image channel.

The ability to incorporate single-molecule fluorescence measurement with SMLM was next utilized to achieve *f*-SRM. By encoding functional information into the spectral responses of environment-sensing fluorescent probes, *f*-SRM transcends the structural information provided by typical SRM techniques and reveals the spatiotemporal distribution of physicochemical parameters with single-molecule sensitivity and nanoscale spatial resolution. As one example, by employing the solvatochromic dye Nile Red to sense local chemical polarity, we revealed nanoscale heterogeneity in the membranes of live mammalian cells. This enabled us to unveil substantial polarity differences between the plasma membrane and the membranes of nanoscale intracellular organelles, a result we determined to be due to differences in local cholesterol levels. With the addition of cholesterol or cholera toxin, we further observed the formation of low-polarity, raftlike nanodomains in the plasma membrane.

In another study, we generalized SR-SMLM to fluorogenic single-molecule reactions. As a wide-field technique, SR-SMLM readily captures the emission spectra of individual product fluorescent molecules that are stochastically produced from nonfluorescent reactants at random locations over large sample areas, and therefore, it provides the unique possibility to spectrally identify and characterize single product molecules in a high-throughput fashion. Using the ring-opening reaction of a photochromic spiropyran as an example, we demonstrated that the capability to resolve the emission spectra of single product molecules could unveil rich, multipath reaction pathways.

In summary, by integrating the spatial, temporal, and spectral dimensions of single-molecule fluorescence, SR-SMLM and *f*-SRM add rich spectral and functional dimensions to SRM and thus open up new ways of probing biological and chemical systems at the single-molecule and nanoscale levels.

1. INTRODUCTION

The diffraction-imposed ∼300 nm resolution limit of light microscopy has been surmounted in the past decade by super-resolution (fluorescence) microscopy/nanoscopy (SRM).[1,2]

Received: October 30, 2017

DOI: 10.1021/acs.accounts.7b00545
Acc. Chem. Res. XXXX, XXX, XXX−XXX

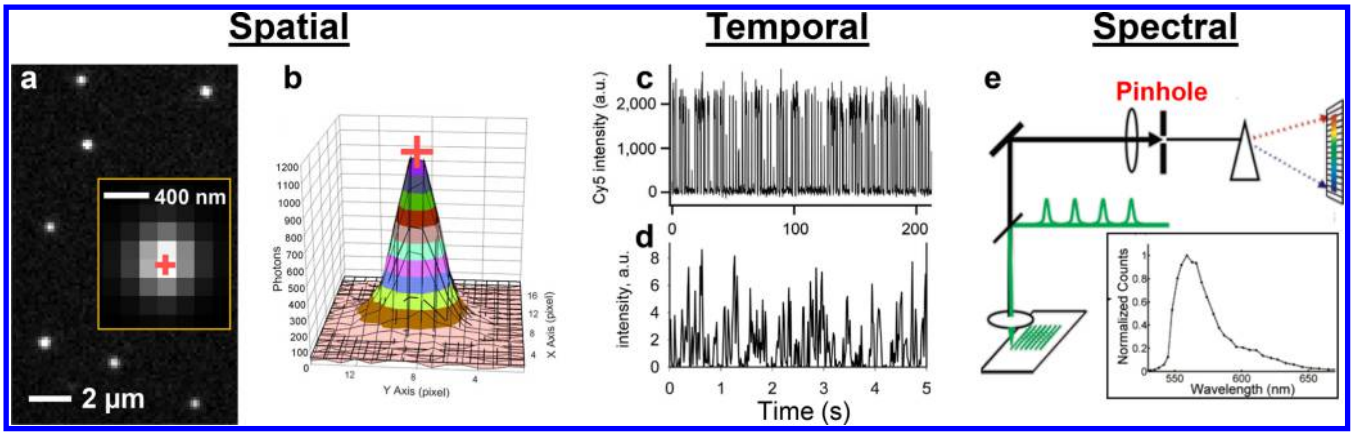

Figure 1. Spatial, temporal, and spectral dimensions of single-molecule fluorescence. (a) Wide-field fluorescence image of single AF647 molecules. (b) Intensity distribution of a Cy3 molecule as recorded by a camera. The red crosses in (a) and (b) mark peak positions. Adapted with permission from ref 10. Copyright 2003 AAAS. (c) Laser-induced reversible fluorescence photoswitching of a Cy3−Cy5 dye pair. Adapted with permission from ref 11 Copyright 2006 Springer Nature. (d) Fluorescence bursts due to the binding/unbinding of single Nile Red molecules to a lipid vesicle. Adapted with permission from ref 14. Copyright 2006 National Academy of Sciences. (e) Scanning-based single-location spectroscopy for single molecules. Adapted from ref 25. Copyright 2005 American Chemical Society.

While offering remarkable spatial resolution of ∼10 nm and profound impacts across multiple research fields,[2−4] SRM typically provides monochrome images. The lack of spectral information complicates efforts of multicolor/multitarget SRM; common approaches rely on false-color superimposition of images obtained from different filter channels, for which image alignment and signal crosstalk are often challenging. Moreover, colorless images convey only spatial information and leave little room beyond structure and shape.

By tapping into the often overlooked yet extremely informative dimension of the fluorescence spectrum, we have recently realized spectrally resolved SRM for highly multiplexed imaging. By encoding functional information into this new spectral dimension with environment-sensing probes, functional SRM further enables the interrogation of local physicochemical parameters at the nanoscale. These remarkable results are achieved by integrating the spatial, temporal, and spectral dimensions of single-molecule fluorescence.

Fluorescence detection provides a noninvasive and target-specific means to probe single molecules.[5−8] Figure 1a shows a typical wide-field fluorescence image of single Alexa Fluor 647 (AF647) molecules. Because of diffraction, single molecules appear as ∼300 nm-sized spots. However, it is recognized that the position of a single molecule can be determined with nanometer precision by fitting the intensity distribution of its image (Figure 1b) to known functions.[9,10] The ability to thus "superlocalize" the position of a molecule is crucial for experiments that utilize spatial information on single molecules.

Time trajectories of intensity represent another important aspect of single-molecule fluorescence. In particular, the integration of on−off intensity dynamics (fluorescence switching; Figure 1c,d) with the aforementioned ability to superlocalize single molecules has led to the invention of a major class of SRM methods generally known as single-molecule localization microscopy (SMLM).[11−13] In one such implementation, stochastic optical reconstruction microscopy (STORM),[11] fluorescent molecules are first photoswitched to a nonemitting state. Small, random subsets of the nonemitting molecules are then photoswitched back to the emitting state (Figure 1c) and superlocalized over different camera frames to construct an SRM image. In another SMLM approach, points accumulation for imaging in nanoscale topography (PAINT),[14] the reversible binding/unbinding of fluorescent molecules to the sample (Figure 1d) is utilized to achieve single-molecule localization. Chemical reactions can also achieve on−off switching via the in situ generation of fluorescent molecules; superlocalizing the product molecules enables super-resolution mapping of local reactivity.[4,8,15]

Spectrum measurement is another key component of single-molecule fluorescence, but one that is also highly challenging. Whereas the recording of total light intensity suffices for examining the spatial and temporal dimensions of single-molecule fluorescence, scrutinizing the spectral dimension necessitates the wavelength-dependent detection of light. The use of a dichroic mirror to split fluorescence into long- and short-wavelength components offers a facile way to estimate the emission wavelengths of single molecules by calculating the intensity ratio of the two components,[16,17] and this "ratiometric" approach has been successfully incorporated with SMLM.[18−20] However, actual spectra are not obtained, and the result is subject to sample background and performance of the dichroic mirror.

To truly resolve single-molecule spectra, previous work has often employed spatially confined illumination and detection for spectral dispersion of the fluorescence from a single spot of the sample.[5,6,21−25] Sample scanning then enables the mapping of the positions and spectra of sparsely distributed molecules at different locations with limited throughput (Figure 1e). Although multiplexed arrays of confined illumination and detection spots have enabled the parallel measurement of single-molecule spectra with high throughput,[26] such approaches are difficult to apply to imaging and still rely on the sparse distribution of molecules.

2. SPECTRALLY RESOLVED SUPER-RESOLUTION MICROSCOPY VIA ULTRAHIGH-THROUGHPUT SINGLE-MOLECULE SPECTROSCOPY

To overcome these limits in the context of SMLM, we reasoned[27] that sparsely distributed single fluorescent molecules are discrete, self-confined point sources (Figure 2a). Consequently, to collect their spectra, it appears unnecessary to impose further spatial confinement in illumination or detection,

DOI: 10.1021/acs.accounts.7b00545
Acc. Chem. Res. XXXX, XXX, XXX−XXX

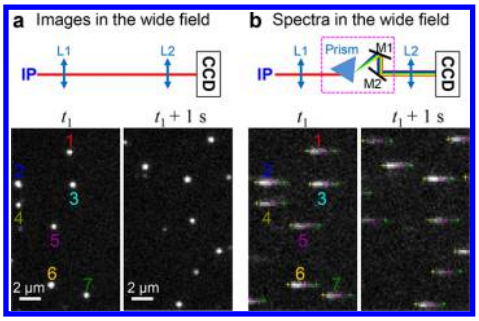

Figure 2. Wide-field fluorescence spectroscopy for single molecules. (a) (top) A wide-field image is relayed through lenses L1 and L2. IP denotes the intermediate image plane of the microscope. (bottom) A small part of the acquired images of single immunolabeled AF647 molecules in a fixed cell in two 9 ms camera frames separated by 1 s. (b) (top) A prism is placed at the Fourier plane between L1 and L2. (bottom) The dispersed spectra for the same molecules in (a) recorded in the wide field concurrently with the images in (a). Yellow, magenta, and green crosses show the spectral positions of 647, 700, and 750 nm for each molecule, mapped on the basis of calibration obtained using narrow-bandpass filters and lasers with known wavelengths. Adapted with permission from ref 27. Copyright 2015 Springer Nature.

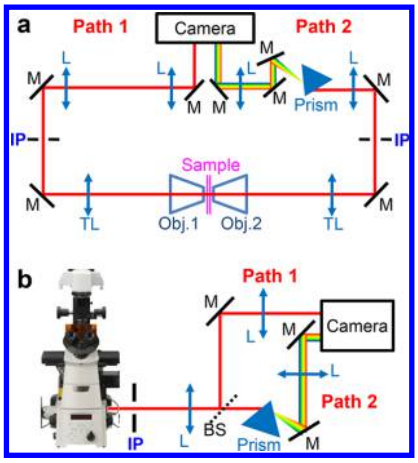

Figure 3. Concurrent positional and spectral measurements of single molecules. (a) System based on two opposing objective lenses. (b) System based on an inverted microscope with a single objective lens. Abbreviations: Obj., objective lens; TL, tube lens; M, mirror; L, lens; BS, beamsplitter; IP, intermediate image plane. For both schemes, paths 1 and 2 provide unmodified images and dispersed spectra of single molecules, respectively.

as done in previous studies. Instead, by means of a prism, the emission of many molecules in the same field of view may be simultaneously dispersed into spectra and recorded with a camera (Figure 2b). Although analogous wide-field spectroscopy approaches are occasionally used in astronomy for stellar spectra,[28] their direct application to single-molecule experiments has been limited to sparse systems.[29,30] We found that through integration of SMLM[11−14] with our wide-field spectroscopy scheme, a few-millisecond snapshot could readily capture the emission spectra of ~10^2 randomly distributed single emitting molecules. Via photoswitching (for STORM) or reversible labeling (for PAINT), we then stochastically lit up different populations of molecules over consecutive camera frames and obtained the spectra of ~10^6 single molecules in a densely labeled sample within minutes. In contrast to previous scanning-based single-location imaging/spectroscopy approaches, in which a few molecules are probed per minute, we deem this wide-field approach "ultrahigh-throughput".

A hidden pitfall of the above wide-field scheme is that the spatial information and spectral information on a randomly located molecule are coupled:[27] the dispersed spectrum of a redder molecule may appear identical to that of a bluer molecule physically located further to the right. An independent reference image is thus necessary to decouple the spatial and spectral dimensions and produce the final result of spectrally resolved SMLM (SR-SMLM, including SR-STORM and SR-PAINT).

In our initial work,[27] we employed a dual-objective scheme in which the sample is sandwiched between two opposing objective lenses, so that separate objectives are dedicated to the positional (Figure 3a, path 1) and spectral (Figure 3a, path 2) measurements of the same single molecules. This design achieves excellent light efficiency: the image channel of path 1 is unmodified compared to regular SMLM setups, whereas the spectral information from path 2 is added on "for free". The major drawback is that samples need to be thin and transparent to allow imaging from the back side, and the mounting geometry is unfavorable for live-cell experiments.

Mlodzianoski et al.[31] reported an SR-SMLM system based on an inverted microscope with a single objective lens. A beamsplitter divides the fluorescence collected by the objective lens into two paths for separate positional and spectral detections of single molecules. We employed a similar strategy (Figure 3b) in our recent work on live cells.[32] Although dividing the signal into two paths reduces the number of photons available for each path, this system imposes fewer sample constraints and is simpler in design.

Recent work has also reported SR-SMLM through concurrent positional and spectral recording via the zeroth and first diffraction orders of a grating,[33,34] a strategy used in earlier single-molecule/single-particle studies.[29,30] Although gratings could in principle provide higher resolving power over prisms and offer the benefit of linear dispersion, they achieve limited light efficiency, which could be a concern given the restricted photon budget for single molecules. Their strong dispersion also reduces the signal-to-noise ratio of each pixel and exacerbates overlap between the dispersed spectra of different molecules, making it difficult to probe densely labeled two-dimensional structures.

Another strategy encodes the spectral information on single molecules into the shape of single-molecule images (point spread functions (PSFs)).[36−38] Although such approaches remove the need for a reference image, they do not provide actual spectra. The spatial light modulator or phase mask involved also limits light-use efficiency. Color separation thus has been demonstrated only for large wavelength differences. Table 1 provides a summary of different approaches and their major limitations.

3. SPECTRALLY RESOLVED SUPER-RESOLUTION MICROSCOPY FOR MULTIPLEXED IMAGING

One immediate application of SR-SMLM is multiplexed SRM. To determine how well different fluorophores can be distinguished, we first characterized the intrinsic spectral variation among individual molecules of the same fluorophore.[27] Previous studies reported substantial spectral variation (standard deviation of ~10 nm) for single dye molecules

DOI: 10.1021/acs.accounts.7b00545
Acc. Chem. Res. XXXX, XXX, XXX−XXX

Table 1. Spectroscopic Approaches for SMLM

method	demonstrated multicolor SMLM	major limitations	ref(s)
ratiometric detection	four fluorophores at ~20 nm spectral separation	spectra not obtained; results subject to dichroic mirror	18−20
dual objective + prism	four fluorophores at ~10 nm spectral separation	thin, transparent samples only	27, 35
beamsplitter + prism	three fluorophores at ~20 nm spectral separation	photons split over two channels	31, 32
diffraction grating	two fluorophores at ~20 nm spectral separation	low light efficiency; signal spread over too many pixels	33, 34
PSF engineering	two fluorophores at >100 nm spectral separation	spectra not obtained; low light efficiency	36

immobilized at solid surfaces (e.g., Figure 4a).[5,21−23] Meanwhile, ratiometric SMLM of dye-labeled biological samples[18,19]

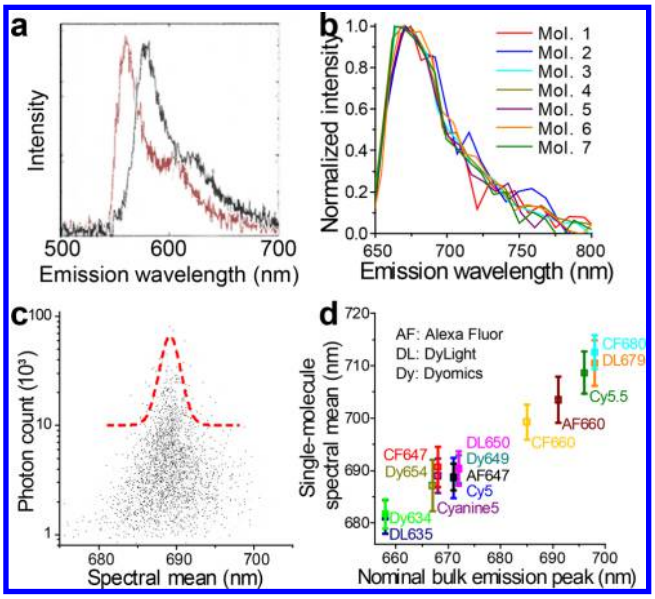

Figure 4. Variation in single-molecule fluorescence spectra. (a) Spectra of two $DiIC_{12}(3)$ molecules at a poly(methyl methacrylate)−air interface. Adapted with permission from ref 22. Copyright 1996 AAAS. (b) Spectra of the individual AF647 molecules labeled as 1−7 in Figure 2. (c) Measured spectral mean vs photon count for 6406 single AF647 molecules detected within 3 s. (d) Single-molecule spectral mean distributions of 14 different dyes, each obtained through SR-STORM from ~10^6 molecules. Error bars represent standard deviations between single molecules. (b−d) Adapted with permission from ref 27. Copyright 2015 Springer Nature.

found relatively high uncertainty in fluorophore identification (~20% crosstalk for 4 dyes at ~20 nm spectral separation), and it was unclear how much of the uncertainty is due to intrinsic spectral variation between single molecules.

Remarkably, with SR-STORM we found that in typical buffers, single immunolabeled dye molecules exhibit highly uniform fluorescence emission in cells (Figure 4b,c).[27] Statistics of the spectral mean, calculated as the intensity-weighted average of wavelengths of each molecule,[23] gave a standard deviation of 2.6 nm for the ~6 × 10^5 individual AF647 molecules detected in the sample shown in Figure 2, with the brighter molecules (>10 000 detected photons) converging to an extremely small standard deviation of 1.4 nm (Figure 4c). Notably, a previous study measured the emission spectra of 220 single AF647 molecules electrokinetically trapped in an aqueous buffer, and it also noted a narrow distribution of emission wavelengths (standard deviation ~3.5 nm).[39] Together, these results suggest that in aqueous buffers, single dye molecules may be characterized by much narrower emission distributions compared with surface-trapped molecules. To generalize this finding, we investigated 14 far-red dyes excited at 647 nm and found homogeneous single-molecule spectra for all (standard deviations of 2.5−4.5 nm in the single-molecule spectral means; Figure 4d). Meanwhile, substantial spectral differences were detected for different dyes (Figure 4d).

Consequently, our method should reliably distinguish single molecules of different dyes that differ minimally in emission spectrum. To show this, we performed SR-STORM on cells in which four distinct subcellular structures were immunolabeled by four 647 nm-excited far-red dyes that were just ~10 nm apart in emission wavelength.[27] By color-coding each detected single molecule according to its measured spectral mean on a continuous scale, we found that in the resultant "true-color" SR-STORM images, molecules of different dyes were readily distinguishable, so that distinct colors showed up for the four differently labeled subcellular structures (Figure 5a). Classification of the spectrum of each single molecule into the four dyes gave excellent separation (Figure 5b) and negligible (≲1%) misidentification (Figure 5c). Meanwhile, locally averaged single-molecule spectra for the different sub-diffraction-limit structures showed good agreement with the spectra of the corresponding dyes (Figure 5d). It is also apparent from Figure 5d that as the emission spectra are so heavily overlapped among the four dyes, color separation would not have been possible with conventional approaches using bandpass filters.

We further integrated our approach with 3D-STORM[40] by encoding depth information into the shape of single-molecule images (Figure 6). The resultant four-dimensional (1D spectral + 3D spatial) information on every molecule allowed us to achieve crosstalk-free four-color 3D SRM in which the 3D images of all four labels were collected in the same coordinates. We thus circumvented the major challenge of aligning different SRM channels in three dimensions, as faced by many traditional approaches. Meanwhile, as the spectral information was provided by a second objective lens, the photon counts and spatial resolution of the image channel remained typical of regular SMLM setups.[27]

4. FUNCTIONAL SUPER-RESOLUTION MICROSCOPY

With the success of SR-SMLM for multiplexed SRM, our next challenge[27] was to further integrate fluorophores that are spectrally responsive to local environments so as to utilize the new spectral dimension of single-molecule fluorescence to probe local functional parameters, giving rise to functional SRM (*f*-SRM). By "functional" we emphasize the possibility to advance beyond the "structural" information available to typical SRM techniques and reveal the spatiotemporal distribution of physicochemical parameters (e.g., chemical polarity, pH, ion concentrations, and viscosity) with nanoscale spatial resolution and single-molecule sensitivity.

Although many fluorescent probes have been developed to report local environments through spectral changes,[41−43]

DOI: 10.1021/acs.accounts.7b00545
Acc. Chem. Res. XXXX, XXX, XXX−XXX

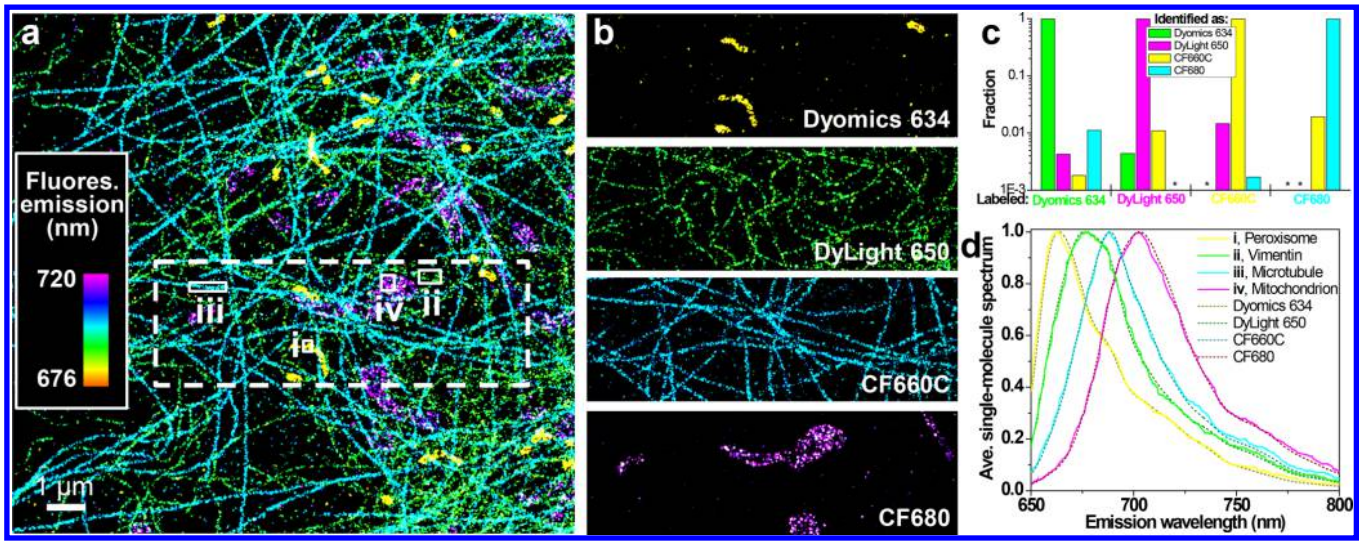

Figure 5. SR-STORM for four-color SRM. (a) "True-color" SR-STORM image of four subcellular targets immunolabeled with four far-red dyes at 10 nm spectral separation. Colors represent the measured spectral means of individual molecules on a continuous scale (inset). (b) Separation of the four dye channels for the dash-boxed area in (a). (c) Identification/misidentification of the four dyes based on the measured single-molecule spectra (asterisks: $< 10^{-3}$) (d) Averaged single-molecule spectra for the different nanoscale subcellular structures (i–iv) marked in (a), compared to those individually measured for the four dye molecules. Adapted with permission from ref 27. Copyright 2015 Springer Nature.

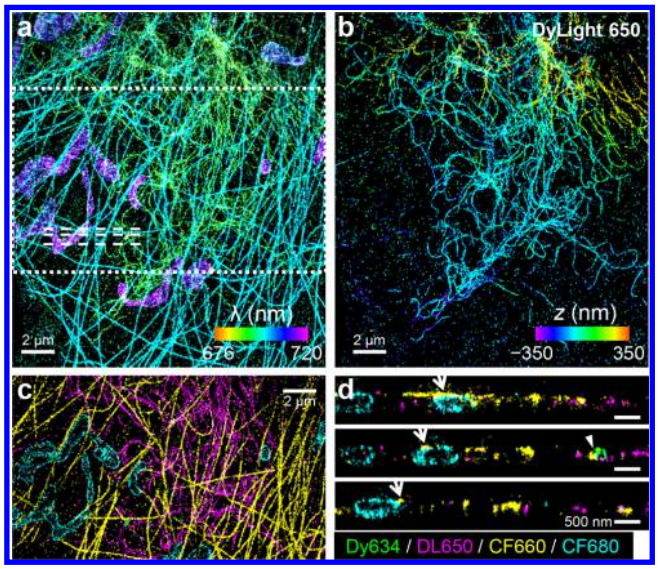

Figure 6. SR-STORM for 3D-SRM. (a) True-color SR-STORM image of a cell similar to that in Figure 5. (b) The isolated channel of one of the four dyes, recolored according to depth (z) (color bar). (c) Virtual in-plane (xy) cross-section for the boxed area in (a), at the center of the mitochondria. Here each molecule is categorized as one of the four dyes and accordingly false-colored. (d) Vertical xz sections along the three dashed lines in (a). Adapted with permission from ref 27. Copyright 2015 Springer Nature.

conventional detection methods provide limited spatial resolution, which in turn leads to reduced sensitivity to local spectral differences. The ability to scrutinize the spectral response of every probe molecule one at a time may help achieve the ultimate sensitivity to the local environment. Earlier, pioneering single-molecule spectral studies of environment-sensing probes were limited to low molecule counts in sparse samples.[16,44] With the ultrahigh throughput of SR-SMLM, it now appears possible to map out functional parameters at the nanoscale with millions of individual probe molecules. The observation that single molecules that are ∼10 nm apart in emission wavelength can be readily distinguished from each other (Figure 5) further suggests high sensitivity.

Bongiovanni et al.[34] combined Nile Red, a solvatochromic dye, with SR-PAINT to enable hydrophobicity mapping of unilamellar lipid vesicles, in vitro protein aggregates, and cell surfaces. However, as the experiments were based on the zeroth and first diffraction orders of a grating (as discussed above), the strong dispersion did not allow probing of dense two-dimensional structures like in-plane views of the cell.

With a prism-based beam-splitting design (Figure 3b), we achieved Nile Red-based SR-STORM and SR-PAINT *f*-SRM for the membranes of live mammalian cells and thus revealed their compositional heterogeneity at the nanoscale.[32] By collecting the spectral and spatial information on ∼10^6 membrane-bound, 561 nm-excited Nile Red molecules, we again assigned a color to each molecule on the basis of its spectral mean (Figure 7). Remarkably, the resultant true-color SRM images revealed striking spectral differences between the plasma membrane and the membranes of intracellular organelles (Figure 7a), and such differences were maintained as the cellular membranes rearranged at the nanoscale (Figure 7bc). The averaged single-molecule spectra were identical for mitochondrial and endoplasmic reticulum membranes but red-shifted by ∼20 nm compared with the plasma membrane (Figure 7d). On the basis of the solvatochromic behavior of Nile Red, the redder spectra of intracellular membranes suggest that they are more polar and thus more flexible and permeable, in agreement with their expected functions.[45] These results are also in line with recent diffraction-limited ratiometric and lifetime imaging studies employing UV- and violet-excited probes of stronger solvatochromic effects.[43,46,47]

We next determined that the striking polarity differences we found for the organelle and plasma membranes were driven by their known disparity[45] in cholesterol level. A comparison with SR-PAINT *f*-SRM results of supported lipid bilayers indicated that the organelle and plasma membranes were spectrally analogous to cholesterol-free and cholesterol-added bilayers, respectively (Figure 7d). In cells, we found that depletion of cholesterol significantly red-shifted single-molecule spectra at

DOI: 10.1021/acs.accounts.7b00545
Acc. Chem. Res. XXXX, XXX, XXX−XXX

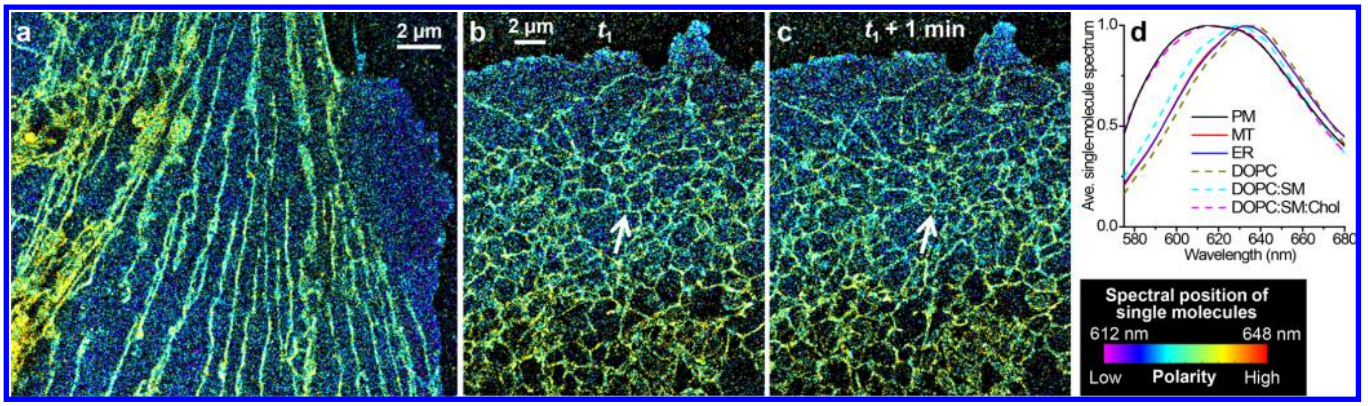

Figure 7. Spectrally resolved *f*-SRM visualizes polarity differences between organelle and plasma membranes in live cells. (a) True-color SR-PAINT image of a Nile Red-labeled PtK2 cell. Each detected single molecule is color-coded according to its spectral mean [color bar below (d)]. (b, c) Sequential true-color SR-STORM images of a Nile Red-labeled COS-7 cell at 1 min separation. Arrows point to structural changes in the endoplasmic reticulum (ER). (d) Averaged spectra of single Nile Red molecules from different nanoscale regions at the plasma membrane (PM), mitochondria (MT), and ER compared to those at supported lipid bilayers of different compositions. Adapted from ref 32. Copyright 2017 American Chemical Society.

the plasma membrane, so that the spectral difference between the plasma membrane and organelle membranes was largely removed, as evidenced by both true-color SRM images (Figure 8a) and locally averaged single-molecule spectra (Figure 8b).

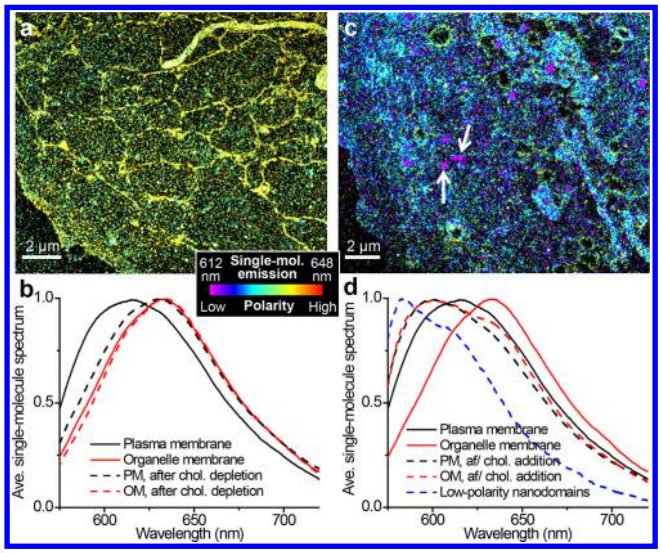

Figure 8. Cholesterol drives polarity heterogeneity in cellular membranes. (a) True-color Nile Red SR-STORM image of a cholesterol-depleted cell. (b) Averaged single-molecule spectra at the plasma membrane (PM) and organelle membrane (OM). (c) True-color Nile Red SR-STORM images of a cholesterol-added cell. Arrows point to low-polarity nanodomains. (d) Averaged single-molecule spectra at the PM, OM, and low-polarity nanodomains. Adapted from ref 32. Copyright 2017 American Chemical Society.

Conversely, addition of cholesterol led to significant blue shifts of all cellular membranes (Figure 8c,d). Together, these results indicate that cholesterol, which is known to play key roles in packing of lipid bilayers into more ordered and less hydrated phases,[45,48] drives the polarity differences we found between the plasma and organelle membranes.

Intriguingly, for cholesterol-added cells, in addition to an overall blue shift, *f*-SRM further revealed nanosized (~100 nm) domains of strongly blue-shifted spectra across the plasma membrane (arrows in Figure 8c). This result suggests the presence of a new, highly nonpolar phase at the nanoscale, reminiscent of the long-hypothesized cholesterol-rich raftlike nanodomains in cell membranes.[48,49] Following this lead, we found that similar low-polarity nanodomains can also be induced by cholera toxin B-subunit (CTB), a common lipid-raft marker and stabilizer. Through comparisons of both *f*-SRM images and the distributions of single-molecule spectra from *f*-SRM data (Figure 9), we further concluded that such low-

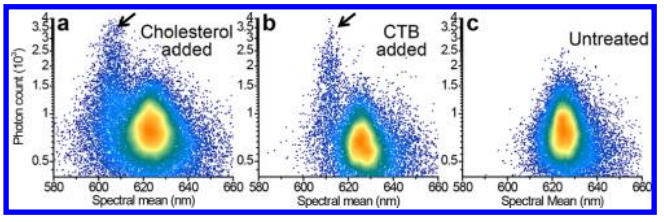

Figure 9. Identifying the low-polarity membrane phase through single-molecule statistics. Distributions of spectral mean and photon count for single Nile Red molecules at the plasma membranes of (a) cholesterol-added, (b) CTB-treated, and (c) control COS-7 cells. Arrows point to molecules in the low-polarity phase. Adapted from ref 32. Copyright 2017 American Chemical Society.

polarity membrane phases are likely absent in untreated native cells. We thus revealed rich nanoscale heterogeneity in live-cell membranes, both between organelle and plasma membranes and within the plasma membrane itself.

5. SPECTRALLY RESOLVED SUPER-RESOLUTION MICROSCOPY REVEALS REACTION PATHWAYS OF SINGLE MOLECULES

The integration of SMLM with the spectral measurement of single molecules has also proven valuable for investigating single-molecule reactions.[35] Recent studies have established fluorescence microscopy as an important tool to study single-molecule chemical reactions.[4,8,15] In particular, for fluorogenic reactions, monitoring when (temporal dimension) and where (spatial dimension) individual fluorescent product molecules are generated has provided rich information on reaction dynamics and enabled reactivity mapping at the super-resolution level. Further incorporating the fluorescence spectrum could provide a powerful means to identify and

DOI: 10.1021/acs.accounts.7b00545
Acc. Chem. Res. XXXX, XXX, XXX−XXX

characterize product molecules. However, as the reactant molecules are often nonfluorescent and thus undetectable before the reaction occurs, it is naturally difficult to follow single-molecule reactions with traditional single-position spectroscopy approaches. In contrast, the wide-field nature of SR-SMLM offers a direct means to capture the fluorescence spectra of single molecules that sporadically switch into the fluorescent state at random locations (Figures 2 and 10) and can thus deliver the missing spectral dimension of single-molecule reactions.

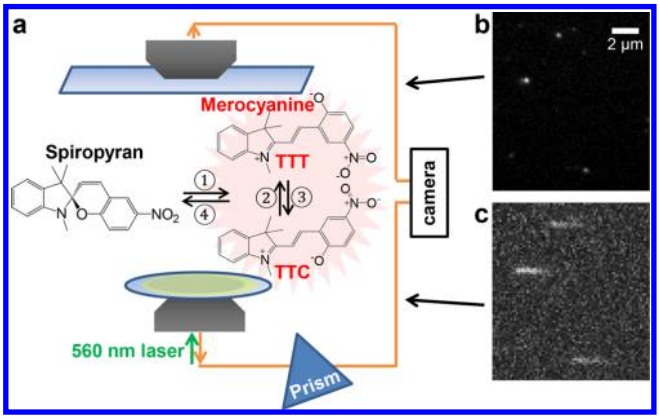

Figure 10. SR-SMLM investigation of the ring-opening (1), ring-closure (4), and cis−trans isomerization (2,3) reactions of single spiropyran molecules. (a) Schematic of the system. (b, c) A small region of the concurrently acquired fluorescence images (b) and spectra (c) of three single product molecules, obtained in a 33 ms snapshot. Adapted from ref 35. Copyright 2017 American Chemical Society.

To demonstrate this possibility, we studied the fluorogenic ring-opening reaction of the photochromic spiropyran 1′,3′-dihydro-1′,3′,3′-trimethyl-6-nitrospiro[2*H*-1-benzopyran-2,2′-(2*H*)-indole] (6-nitro-BIPS).[35] This reaction generates two major fluorescent cis−trans merocyanine isomers, TTC and TTT (Figure 10a),[50] but with bulk measurements it is difficult to separate their respective spectral contributions to the product mixture.

With SR-SMLM, we obtained the spectra and locations of thousands of individual fluorescent product molecules stochastically generated from the ring opening of surface-adsorbed 6-nitro-BIPS (Figure 10). Remarkably, we identified two populations that were comparable in brightness but distinct in spectral mean (Figure 11a−c) and spectrum (Figure 11d), attributable to the TTC and TTT isomers. Moreover, we found a strong solvent polarity dependence for the relative population of the two products (Figure 11a−c,e), signifying the importance of the solvent in determining the reaction pathway.

By examining the spectral time traces of individual molecules, we next identified various single-molecule reaction processes, including stable isomers (Figure 12a), isomerization between the two isomers (Figure 12b,c), ring-closure reaction back to the spiropyran form (Figure 12d,e), and more complex behaviors involving multiple processes (Figure 12f). For these results, the ability to superlocalize single molecules with high precision was instrumental in ascribing multiple fluorescence signals to the same molecule. We thus demonstrated that the spectrum-resolving capability of SR-SMLM could unveil rich multipath pathways for single-molecule reactions.

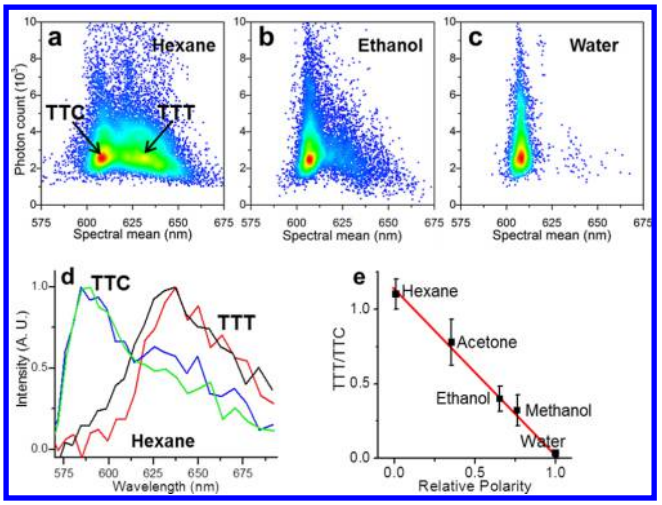

Figure 11. Statistics of single-molecule spectra revealing two spectrally distinct products for the ring opening of 6-nitro-BIPS. (a−c) Distribution of the measured single-molecule spectral means and photon counts in *n*-hexane, ethanol, and water. (d) Representative single-molecule spectra of the two isomers in *n*-hexane. (e) Dependence of the TTT/TTC ratio on the solvent polarity. Adapted from ref 35. Copyright 2017 American Chemical Society.

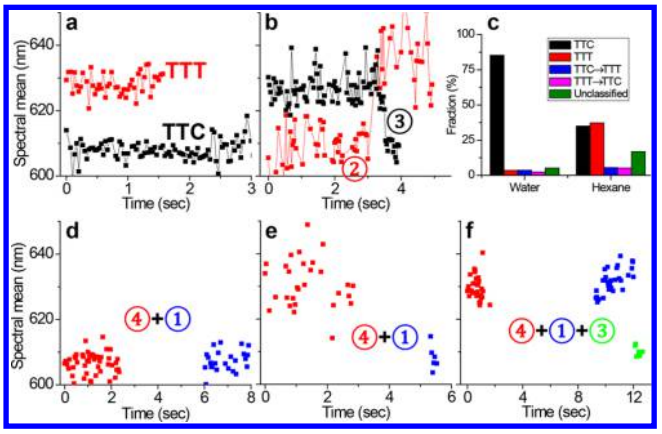

Figure 12. Monitoring the reaction pathways of single molecules through spectral time traces. (a) Time traces for two spectrally unvarying TTC (black) and TTT (red) product molecules. (b) Time traces showing TTC → TTT (red) and TTT → TTC (black) isomerizations. (c) Statistics of ∼1000 single-molecule spectral time traces in water and hexane as stable isomers or isomerization processes. (d−f) Time traces involving reversible on/off single-molecule fluorescence switching attributable to ring closure. Circled numbers in (b) and (d−f) correspond to the different reaction pathways in Figure 10a. Adapted from ref 35. Copyright 2017 American Chemical Society.

6. CONCLUSION AND OUTLOOK

By integrating the spatial, temporal, and spectral dimensions of single-molecule fluorescence through a wide-field scheme, our SR-SMLM approach has merged and expanded the capabilities of SRM and single-molecule spectroscopy.

For multiplexed SRM, as we have achieved near-zero color crosstalk among four far-red dyes that are ∼10 nm apart in emission wavelength, it is conceivable that more fluorophores may be included in the same far-red emission window (to be excited by a single red laser) at the expense of modest crosstalk between channels. The combination of different excitation lasers (we have so far demonstrated 560 and 647 nm) could

DOI: 10.1021/acs.accounts.7b00545
Acc. Chem. Res. XXXX, XXX, XXX−XXX

enable even more color channels over wider spectral windows, although attempts to record too many dyes simultaneously could make it difficult to achieve the desired single-molecule sparsity.

For *f*-SRM, we have shown how measuring the fluorescence spectra of millions of polarity-sensing single molecules can reveal nanoscale compositional heterogeneity in live-cell membranes. The ultimate sensitivity achieved through scrutinizing the spectral response of individual molecules may also be harnessed to probe other parameters (e.g., local pH, viscosity, and protein activity) in cells and other biological and nonbiological systems. Major challenges in exploring these possibilities lie in the identification or construction of suitable fluorescent probes that are both environmentally sensitive and SMLM-compatible. Meanwhile, the specific tagging of sensing fluorophores to target (bio)molecules would be highly valuable in constraining environment probing to specific (subcellular) structures. Correlative approaches[3] integrating *f*-SRM with other microscopy and spectroscopy tools would further expand the horizons.

For single-molecule reactions, we have demonstrated SR-SMLM as a powerful tool for resolving the multipath reaction pathways of single spiropyran molecules. The ability to capture the spectra of randomly generated single fluorescent molecules over large areas may also be utilized to study other reactions and dynamic processes. For now, however, applications may be restricted to processes involving bright fluorescent molecules, and the achievable time resolution is limited to milliseconds.

In conclusion, by adding remarkably rich spectral and functional dimensions to the already powerful SRM, spectrally resolved and functional SRM opens up exciting new ways to probe biological and chemical systems at the single-molecule and nanoscale levels. We look forward to the continued development of related methods as well as their application to a broad spectrum of research fields and scientific questions.

AUTHOR INFORMATION

Corresponding Author

*E-mail: xuk@berkeley.edu.

ORCID

Rui Yan: 0000-0003-3391-133X
Ke Xu: 0000-0002-2788-194X

Author Contributions

[‖]R.Y., S.M., and S.J.K. contributed equally.

Notes

The authors declare no competing financial interest.

Biographies

Rui Yan obtained a B.S. in biology from Peking University, where he studied DNA repair mechanisms and inflammatory pathways. He joined the Xu group in 2015 as a graduate student. His research interests include interrogation of biological issues with functional super-resolution microscopy.

Seonah Moon received her B.S in chemistry from Korea Advanced Institute of Science and Technology, where she studied ultrafast exciton dynamics of polymer solar cell materials. She joined the Xu group in 2014. Her research interests include the application of functional super-resolution microscopy to live cells to understand chemical heterogeneities at the nanoscale.

Samuel J. Kenny received his B.S. in chemistry from the University of Minnesota, where he studied nonlinear dynamics of coupled chemical oscillators. He joined the Xu group in 2013. His research interests include the development of multicolor super-resolution microscopy and image analysis methodologies.

Ke Xu received his B.S. in chemistry from Tsinghua University and obtained a Ph.D. in chemistry from the California Institute of Technology. After postdoctoral work at Harvard University, he joined the Department of Chemistry at the University of California, Berkeley, as an assistant professor in 2013. His current work develops new physicochemical tools for biological and chemical research by integrating microscopy, spectroscopy, nanomaterials, and cell biology.

ACKNOWLEDGMENTS

We thank all past and current lab members for contributions and Professor Stephen Leone for comments. This work was supported by the Beckman Young Investigator Program, the National Science Foundation (CHE-1554717), the Packard Fellowships for Science and Engineering, and the Bakar Fellows Award. K.X. is a Chan Zuckerberg Biohub investigator and acknowledges additional support from STROBE, an NSF Science and Technology Center (DMR-1548924). S.M. acknowledges a Samsung Scholarship.

REFERENCES

(1) Huang, B.; Bates, M.; Zhuang, X. Super-resolution fluorescence microscopy. *Annu. Rev. Biochem.* **2009**, *78*, 993−1016.

(2) Sahl, S. J.; Hell, S. W.; Jakobs, S. Fluorescence nanoscopy in cell biology. *Nat. Rev. Mol. Cell Biol.* **2017**, *18*, 685−701.

(3) Hauser, M.; Wojcik, M.; Kim, D.; Mahmoudi, M.; Li, W.; Xu, K. Correlative super-resolution microscopy: new dimensions and new opportunities. *Chem. Rev.* **2017**, *117*, 7428−7456.

(4) Chen, T.; Dong, B.; Chen, K.; Zhao, F.; Cheng, X.; Ma, C.; Lee, S.; Zhang, P.; Kang, S. H.; Ha, J. W.; Xu, W.; Fang, N. Optical super-resolution imaging of surface reactions. *Chem. Rev.* **2017**, *117*, 7510−7537.

(5) Xie, X. S.; Trautman, J. K. Optical studies of single molecules at room temperature. *Annu. Rev. Phys. Chem.* **1998**, *49*, 441−480.

(6) Moerner, W. E.; Orrit, M. Illuminating single molecules in condensed matter. *Science* **1999**, *283*, 1670−1676.

(7) Joo, C.; Balci, H.; Ishitsuka, Y.; Buranachai, C.; Ha, T. Advances in single-molecule fluorescence methods for molecular biology. *Annu. Rev. Biochem.* **2008**, *77*, 51−76.

(8) Cordes, T.; Blum, S. A. Opportunities and challenges in single-molecule and single-particle fluorescence microscopy for mechanistic studies of chemical reactions. *Nat. Chem.* **2013**, *5*, 993−999.

(9) Thompson, R. E.; Larson, D. R.; Webb, W. W. Precise nanometer localization analysis for individual fluorescent probes. *Biophys. J.* **2002**, *82*, 2775−2783.

(10) Yildiz, A.; Forkey, J. N.; McKinney, S. A.; Ha, T.; Goldman, Y. E.; Selvin, P. R. Myosin V walks hand-over-hand: Single fluorophore imaging with 1.5-nm localization. *Science* **2003**, *300*, 2061−2065.

(11) Rust, M. J.; Bates, M.; Zhuang, X. Sub-diffraction-limit imaging by stochastic optical reconstruction microscopy (STORM). *Nat. Methods* **2006**, *3*, 793−795.

(12) Betzig, E.; Patterson, G. H.; Sougrat, R.; Lindwasser, O. W.; Olenych, S.; Bonifacino, J. S.; Davidson, M. W.; Lippincott-Schwartz, J.; Hess, H. F. Imaging intracellular fluorescent proteins at nanometer resolution. *Science* **2006**, *313*, 1642−1645.

(13) Hess, S. T.; Girirajan, T. P. K.; Mason, M. D. Ultra-high resolution imaging by fluorescence photoactivation localization microscopy. *Biophys. J.* **2006**, *91*, 4258−4272.

(14) Sharonov, A.; Hochstrasser, R. M. Wide-field subdiffraction imaging by accumulated binding of diffusing probes. *Proc. Natl. Acad. Sci. U. S. A.* **2006**, *103*, 18911−18916.

DOI: 10.1021/acs.accounts.7b00545
Acc. Chem. Res. XXXX, XXX, XXX−XXX

(15) Chen, P.; Zhou, X.; Andoy, N. M.; Han, K. S.; Choudhary, E.; Zou, N.; Chen, G.; Shen, H. Spatiotemporal catalytic dynamics within single nanocatalysts revealed by single-molecule microscopy. *Chem. Soc. Rev.* **2014**, *43*, 1107−1117.
(16) Brasselet, S.; Moerner, W. E. Fluorescence behavior of single-molecule pH-sensors. *Single Mol.* **2000**, *1*, 17−23.
(17) Tinnefeld, P.; Herten, D. P.; Sauer, M. Photophysical dynamics of single molecules studied by spectrally-resolved fluorescence lifetime imaging microscopy (SFLIM). *J. Phys. Chem. A* **2001**, *105*, 7989−8003.
(18) Bossi, M.; Folling, J.; Belov, V. N.; Boyarskiy, V. P.; Medda, R.; Egner, A.; Eggeling, C.; Schonle, A.; Hell, S. W. Multicolor far-field fluorescence nanoscopy through isolated detection of distinct molecular species. *Nano Lett.* **2008**, *8*, 2463−2468.
(19) Testa, I.; Wurm, C. A.; Medda, R.; Rothermel, E.; von Middendorf, C.; Folling, J.; Jakobs, S.; Schonle, A.; Hell, S. W.; Eggeling, C. Multicolor fluorescence nanoscopy in fixed and living cells by exciting conventional fluorophores with a single wavelength. *Biophys. J.* **2010**, *99*, 2686−2694.
(20) Gunewardene, M. S.; Subach, F. V.; Gould, T. J.; Penoncello, G. P.; Gudheti, M. V.; Verkhusha, V. V.; Hess, S. T. Superresolution imaging of multiple fluorescent proteins with highly overlapping emission spectra in living cells. *Biophys. J.* **2011**, *101*, 1522−1528.
(21) Trautman, J. K.; Macklin, J. J.; Brus, L. E.; Betzig, E. Near-field spectroscopy of single molecules at room-temperature. *Nature* **1994**, *369*, 40−42.
(22) Macklin, J. J.; Trautman, J. K.; Harris, T. D.; Brus, L. E. Imaging and time-resolved spectroscopy of single molecules at an interface. *Science* **1996**, *272*, 255−258.
(23) Lu, H. P.; Xie, X. S. Single-molecule spectral fluctuations at room temperature. *Nature* **1997**, *385*, 143−146.
(24) Moerner, W. E.; Fromm, D. P. Methods of single-molecule fluorescence spectroscopy and microscopy. *Rev. Sci. Instrum.* **2003**, *74*, 3597−3619.
(25) Luong, A. K.; Gradinaru, G. C.; Chandler, D. W.; Hayden, C. C. Simultaneous time- and wavelength-resolved fluorescence microscopy of single molecules. *J. Phys. Chem. B* **2005**, *109*, 15691−15698.
(26) Lundquist, P. M.; Zhong, C. F.; Zhao, P.; Tomaney, A. B.; Peluso, P. S.; Dixon, J.; Bettman, B.; Lacroix, Y.; Kwo, D. P.; McCullough, E.; Maxham, M.; Hester, K.; McNitt, P.; Grey, D. M.; Henriquez, C.; Foquet, M.; Turner, S. W.; Zaccarin, D. Parallel confocal detection of single molecules in real time. *Opt. Lett.* **2008**, *33*, 1026−1028.
(27) Zhang, Z.; Kenny, S. J.; Hauser, M.; Li, W.; Xu, K. Ultrahigh-throughput single-molecule spectroscopy and spectrally resolved super-resolution microscopy. *Nat. Methods* **2015**, *12*, 935−938.
(28) Howell, S. B. Spectroscopy with CCDs. In *Handbook of CCD Astronomy*, 2nd ed.; Cambridge University Press: Cambridge, U.K., 2006; pp 135−166.
(29) Ma, Y.; Shortreed, M. R.; Yeung, E. S. High-throughput single-molecule spectroscopy in free solution. *Anal. Chem.* **2000**, *72*, 4640−4645.
(30) Wei, L.; Liu, C.; Chen, B.; Zhou, P.; Li, H.; Xiao, L.; Yeung, E. S. Probing single-molecule fluorescence spectral modulation within individual hotspots with subdiffraction-limit image resolution. *Anal. Chem.* **2013**, *85*, 3789−3793.
(31) Mlodzianoski, M. J.; Curthoys, N. M.; Gunewardene, M. S.; Carter, S.; Hess, S. T. Super-resolution imaging of molecular emission spectra and single molecule spectral fluctuations. *PLoS One* **2016**, *11*, e0147506.
(32) Moon, S.; Yan, R.; Kenny, S. J.; Shyu, Y.; Xiang, L.; Li, W.; Xu, K. Spectrally resolved, functional super-resolution microscopy reveals nanoscale compositional heterogeneity in live-cell membranes. *J. Am. Chem. Soc.* **2017**, *139*, 10944−10947.
(33) Dong, B. Q.; Almassalha, L.; Urban, B. E.; Nguyen, T. Q.; Khuon, S.; Chew, T. L.; Backman, V.; Sun, C.; Zhang, H. F. Super-resolution spectroscopic microscopy via photon localization. *Nat. Commun.* **2016**, *7*, 12290.
(34) Bongiovanni, M. N.; Godet, J.; Horrocks, M. H.; Tosatto, L.; Carr, A. R.; Wirthensohn, D. C.; Ranasinghe, R. T.; Lee, J. E.; Ponjavic, A.; Fritz, J. V.; Dobson, C. M.; Klenerman, D.; Lee, S. F. Multi-dimensional super-resolution imaging enables surface hydrophobicity mapping. *Nat. Commun.* **2016**, *7*, 13544.
(35) Kim, D.; Zhang, Z.; Xu, K. Spectrally resolved super-resolution microscopy unveils multipath reaction pathways of single spiropyran molecules. *J. Am. Chem. Soc.* **2017**, *139*, 9447−9450.
(36) Shechtman, Y.; Weiss, L. E.; Backer, A. S.; Lee, M. Y.; Moerner, W. E. Multicolour localization microscopy by point-spread-function engineering. *Nat. Photonics* **2016**, *10*, 590−594.
(37) Broeken, J.; Rieger, B.; Stallinga, S. Simultaneous measurement of position and color of single fluorescent emitters using diffractive optics. *Opt. Lett.* **2014**, *39*, 3352−3355.
(38) Smith, C.; Huisman, M.; Siemons, M.; Grunwald, D.; Stallinga, S. Simultaneous measurement of emission color and 3D position of single molecules. *Opt. Express* **2016**, *24*, 4996−5013.
(39) Wang, Q.; Moerner, W. E. Lifetime and spectrally resolved characterization of the photodynamics of single fluorophores in solution using the anti-Brownian electrokinetic trap. *J. Phys. Chem. B* **2013**, *117*, 4641−4648.
(40) Huang, B.; Wang, W.; Bates, M.; Zhuang, X. Three-dimensional super-resolution imaging by stochastic optical reconstruction microscopy. *Science* **2008**, *319*, 810−813.
(41) Han, J.; Burgess, K. Fluorescent indicators for intracellular pH. *Chem. Rev.* **2010**, *110*, 2709−2728.
(42) Yang, Z.; Cao, J.; He, Y.; Yang, J. H.; Kim, T.; Peng, X.; Kim, J. S. Macro-/micro-environment-sensitive chemosensing and biological imaging. *Chem. Soc. Rev.* **2014**, *43*, 4563−4601.
(43) Klymchenko, A. S. Solvatochromic and fluorogenic dyes as environment-sensitive probes: design and biological applications. *Acc. Chem. Res.* **2017**, *50*, 366−375.
(44) Hou, Y.; Bardo, A. M.; Martinez, C.; Higgins, D. A. Characterization of molecular scale environments in polymer films by single molecule spectroscopy. *J. Phys. Chem. B* **2000**, *104*, 212−219.
(45) van Meer, G.; Voelker, D. R.; Feigenson, G. W. Membrane lipids: where they are and how they behave. *Nat. Rev. Mol. Cell Biol.* **2008**, *9*, 112−124.
(46) Golfetto, O.; Hinde, E.; Gratton, E. Laurdan fluorescence lifetime discriminates cholesterol content from changes in fluidity in living cell membranes. *Biophys. J.* **2013**, *104*, 1238−1247.
(47) Niko, Y.; Didier, P.; Mely, Y.; Konishi, G.; Klymchenko, A. S. Bright and photostable push-pull pyrene dye visualizes lipid order variation between plasma and intracellular membranes. *Sci. Rep.* **2016**, *6*, 18870.
(48) Klymchenko, A. S.; Kreder, R. Fluorescent probes for lipid rafts: From model membranes to living cells. *Chem. Biol.* **2014**, *21*, 97−113.
(49) Lingwood, D.; Simons, K. Lipid rafts as a membrane-organizing principle. *Science* **2010**, *327*, 46−50.
(50) Nuernberger, P.; Ruetzel, S.; Brixner, T. Multidimensional electronic spectroscopy of photochemical reactions. *Angew. Chem., Int. Ed.* **2015**, *54*, 11368−11386.

DOI: 10.1021/acs.accounts.7b00545
Acc. Chem. Res. XXXX, XXX, XXX−XXX